Thermotropic Chiral Nematic Side-Chain Polymers and Cyclic Oligomers

Low-Molar-Mass Liquid Crystals

Liquid crystals (LC's) represent a state-of-matter intermediate between a solid crystal and an isotropic liquid. A liquid crystal flows like an ordinary liquid, while other properties, such as optical and dielectric anisotropies, resemble those of a crystalline solid.[1] In general, a somewhat rigid and anisomeric molecular shape (e.g., cylindrical, lath-like, or disc-like) is conducive to the realization of an LC state.[2] Depending on whether temperature or concentration is the dominant factor in inducing mesomorphism, liquid crystals are generally classified into thermotropics and lyotropics.[1,3] Numerous mesophases have been discovered, and they are roughly categorized as follows:

(a) *Nematic mesophase*, where the molecules are aligned with their long axes parallel to each other. Macroscopically, a preferred direction is defined by the "director." The extent to which the molecules are aligned with the director is characterized by the order parameter *S*, defined as

$$S = \frac{1}{2}\left\langle 3\cos^2\theta - 1\right\rangle, \tag{1}$$

where θ is the angle between the long axis of an individual molecule and the director, and $\langle\ \rangle$ represents an average over all molecules present.

(b) *Chiral nematic* or *cholesteric mesophase*, which can be thought of as a stack of nematic layers with their directors rotated at a constant angle either clockwise or counterclockwise from one layer to the next. This spatial variation of the director leads to a helical structure in addition to a long-range orientational order, as in the nematic mesophase.

(c) *Smectic mesophase*, where the molecules exhibit not only a longitudinal order, as in the nematic mesophase, but also a lateral arrangement.

Although the existence of liquid crystals has been recognized for over a century, it is only in the past few decades that their unique linear and nonlinear optical properties have been actively explored for various applications.[4–10] The need to develop LC materials for these applications has been the main driving force behind LC research in recent years. There are basically three device concepts: (a) based on the change in molecular orientation with an applied field, LC's find use as electro-optic devices with response times of the order of a millisecond; (b) appropriate functional moieties allow LC's to respond to electrical or optical stimuli with much shorter response times, i.e., nano- to pico- and even femtosecond, thereby enabling LC's to be employed as fast active devices; (c) LC's have also been extensively explored for passive device applications in which no switching is involved, such as wave plates, polarizers, notch filters, etc.

Molecular-Level Understanding of Cholesteric Mesomorphism

In a comprehensive review article, Solladié and Zimmermann[11] presented a critical appraisal of the issues of helical sense and twisting power underlying the cholesteric mesophase. Two different approaches to the induction of cholesteric mesophase were discussed. Baessler and Labes[12] used chiral compounds that form cholesteric mesophase by themselves, while Stegemeyer and Mainusch[13] employed nematic hosts with chiral dopants. Despite the intensive research devoted previously to the issues of handedness and twisting power, the roles played by chemical structure, including molecular chirality, have remained as challenging as ever.[14] Current understanding of the cholesteric mesophase is summarized as follows:

(a) Helical sense does not correlate with the sign of the specific optical rotation or the absolute configuration of the chiral dopant. Furthermore, it has been demonstrated that inversion of helical sense may occur as a consequence of heating,[15] presumably due to the thermally induced dynamics of conformational isomerism.

(b) Inversion of molecular chirality leads to an opposite handedness at the supramolecular level, but handedness is still not understood in an absolute sense.

(c) A measure of a chiral dopant's ability to induce cholesteric mesophase formation in a nematic host, helical twisting power is strongly dependent on the nematic structure for a given chiral dopant. "Structural similarity" between the nematogenic and chiral components tends to increase helical twisting power.

(d) Helical sense has proven to be very sensitive to structural variations. For cholesteric LC's derived from sterols, the helical sense–chemical structure relationship was interpreted by Baessler and Labes.[12] For nonsteroid materials, the effect of moving the chiral center relative to the neighboring ring, aromatic or alicyclic, of the core structure can be correlated in terms of the SOL/SED and ROD/REL rules;[16,17] however, exceptions to this empiricism have been reported.[18,19]

(e) While there exist no molecular theories capable of treating helical sense at present, chiral/nematic molecular interaction models proposed by Gottarelli *et al.*[20,21] and Rinaldi *et al*.[22–24] could help to elucidate the experimentally observed handedness.

(f) Chilaya and Lisetski[25] indicated that practical applications of existing theories have been hampered by the use of many model parameters that are hard to relate to the properties of real molecules, which is still true in light of more recent approaches.[26–28]

In short, molecular-level understanding of cholesteric mesophase is still lacking at the present time, although a significant amount of empirical information on structure-property relationships has been accumulated over the years. Besides molecular theories,[25–29] computer-aided molecular modeling has been used to gain fundamental insight into LC mesomorphism. Indeed, considerable advances in computer simulation of nematic and smectic mesophases have been made in recent years.[30–33] Memmer *et al*. demonstrated cholesteric mesomorphism using Monte Carlo simulation with the Gay-Berne intermolecular potential function with cubic periodic[34] and twisted[35] boundary conditions. In addition, using the extended-atom approximation, Wilson and Dunmur[36] performed bimolecular modeling of simplified chemical structures aimed at corroborating empirical rules regarding handedness as proposed by Gray *et al*.[16]

Optical Properties of Chiral Nematics

With a longitudinal molecular alignment and the associated optical birefringence, Δn, nematic LC's are well-suited for the fabrication of wave plates to accomplish polarization control. Since optical retardance increases with increasing birefringence for a given thickness, LC's with higher birefringence values call for thinner films in which a higher degree of mesogenic order can be achieved. Nematic alignment also provides an added advantage to second- and third-order nonlinear optical applications where mesogenic cores are nonlinear optically active. The ability to form stable glass with a glass transition temperature T_g above the ambient further enhances the potential for practical applications.

The helical structure underlying the cholesteric mesophase can be characterized by both the helical pitch and its handedness. Helical pitch is defined as the distance along the helical axis over which the director rotates by 360°, and handedness describes the direction in which helical twisting occurs. Depending on the chiral nature of the perturbation, both right- and left-handed helices are possible. The helical structure gives rise to two identifiable textures: focal conic and Grandjean.[36] In focal conic texture, the helical axes are parallel to the substrate surface; whereas in Grandjean texture, the axes are perpendicular to the substrate surface. The Grandjean texture is particularly important because it can reflect incident light over a selective wavelength region. Moreover, this selective reflectivity is accompanied by circular polarization of light, serving as the basis of high-efficiency polarization.[7]

According to well-established theories, the selective reflection wavelength λ_R of a cholesteric LC is governed by the following equation:[37,38]

$$\lambda_R = n_{\text{avg}}\, p\, \cos\theta, \tag{2}$$

where p is the pitch length, θ is the angle of incidence, and n_{avg} is the average refractive index defined as

$$n_{\text{avg}} = \frac{1}{2}\left(n_e + n_0\right), \tag{3}$$

with n_e and n_0 representing extraordinary and ordinary indices of refraction, respectively, of the nematic layers. It has been shown[39] that the bandwidth of selective reflection $\Delta\lambda$ is related to other optical parameters by

$$\Delta\lambda = \lambda_R \frac{\Delta n}{n_{\text{avg}}}, \tag{4}$$

where the optical birefringence Δn is defined as n_e–n_0. Another parameter of interest to molecular design is the so-called helical twisting power (HTP), defined as[40]

$$\mathrm{HTP} = \left(\frac{dp}{dx_{\mathrm{ch}}}\right)_{x_{\mathrm{ch}}\to 0}, \tag{5}$$

and represents the ability of a chiral group to induce cholesteric mesomorphism in a nematic host. Note that higher HTP values require less chiral dopant, in mole fraction, x_{ch}, to yield the same λ_R value. Selective reflection bandwidth $\Delta\lambda$ is another optical parameter of interest to molecular design.

Factors Contributing to Enhanced Optical Birefringence and Selective Wavelength Reflection Bandwidth

Optical birefringence and selective reflection bandwidth are among the molecular design criteria of chiral nematics. From Eqs. (3) and (4) it is clear that bandwidth $\Delta\lambda$ depends on refractive indices n_e and n_0 at a given λ_R. The refractive indices of a uniaxial LC are governed by the LC molecular structure, wavelength, and temperature. Typically, n_0 falls within 1.50±0.04 in the visible spectral region and is weakly dependent on molecular structure. On the other hand, n_e is strongly dependent on molecular structure. Its value varies from about 1.5 for completely saturated compounds to about 1.9 for highly conjugated LC's.[5,38,41,42] Therefore, one can obtain Eq. (6) by differentiating Eq. (4) while keeping n_0 constant:

$$\delta\Delta\lambda \cong \frac{\lambda_R n_0}{n_{\mathrm{avg}}^2}\,\delta\Delta n. \tag{6}$$

Apparently, Δn plays a dominant role in determining the $\Delta\lambda$ value, even though n_{avg} also increases slightly with increasing Δn. This suggests that to achieve a broad selective reflection band, high birefringence nematic and chiral moieties are desired. In what follows, the parameters contributing to an enhanced Δn in nematic layers constituting the cholesteric mesophase will be identified for assessment.

In theory, the optical birefringence of a nematic LC is determined by[43]

$$\Delta n = G(T)\frac{\lambda^2\lambda^{*2}}{\lambda^2 - \lambda^{*2}}, \tag{7}$$

in which

$$G(T) = gNZS\left(f_{\parallel}^{*} - f_{\perp}^{*}\right), \tag{8}$$

where g is a proportionality constant independent of the LC material, N the number of molecules per unit volume, Z the average number of active electrons per LC molecule, S the order parameter, and $\left(f_{\parallel}^{*} - f_{\perp}^{*}\right)$ the differential oscillator strength at the mean resonance wavelength λ^{*}. The factors affecting Δn are analyzed below:

(a) N represents the packing density of LC molecules. A short carbon chain (or short spacer in LCP's) and a large intermolecular force will yield a large birefringence value because of an increased N value. Nevertheless, the ability to increase N to an appreciable extent via molecular design is rather limited.

(b) Z is the average number of active electrons. Three types of electronic transition in organic molecules contribute to Δn: $\sigma \to \sigma^{*}$, $n \to \pi^{*}$, and $\pi \to \pi^{*}$. The $\pi \to \pi^{*}$ transition, representing an excitation of π-electrons, is the most commonly encountered in LC molecules with unsaturated bonds and is the primary contributor to an increased Δn. Increasing the conjugation length or the number of delocalized π-electrons in an LC molecule is therefore a very effective method of enhancing its optical birefringence.

(c) The mean resonance frequency λ^{*} is closely related to the UV absorption spectrum of an LC molecule. From Eq. (7), λ^{*} appears to present a significant effect on Δn. As a consequence, λ^{*} can be increased by increasing the conjugation length.

(d) $\left(f_{\parallel}^{*} - f_{\perp}^{*}\right)$ represents absorption anisotropy. The larger the $\left(f_{\parallel}^{*} - f_{\perp}^{*}\right)$ factor, the greater the Δn value; however, the relationship between $\left(f_{\parallel}^{*} - f_{\perp}^{*}\right)$ and molecular structure is not well understood at this point.

(e) Order parameter S is a function of molecular structure, temperature, and surface alignment. The temperature dependence of S in a nematic mesophase follows:

$$S \cong \left(1 - \frac{T}{T_c}\right)^{\beta}, \tag{9}$$

where T is the temperature, T_c is the nematic-isotropic transition temperature (or clearing temperature), and β is a material constant. Thus, the temperature dependence

of Δn originates primarily in the temperature dependence of S. Furthermore, a higher Δn value will result from a lower processing temperature under otherwise identical conditions.

From the above analysis, it is concluded that the number of delocalized π-electrons plays a major role in achieving high optical birefringence in nematics and, as a result, a broad selective reflection band in cholesterics. However, diminishing solubility in common solvents and bathochromic shift into the visible region impose a limit to which the conjugation length can be increased in favor of optical birefringence. On the other hand, it is anticipated that saturated ring systems are desirable for low optical birefringence and hence a narrow selective reflection band.

Mesophase Fixation via Vitrification, *In-Situ* Polymerization, or Crosslinking

In the applications based on both active and passive device concepts in which field-induced molecular orientation is not involved, it is advantageous to maintain mesomorphic ordering over a long period of time. Various methodologies have been explored to overcome the problems arising from the sensitivity of helical pitch to variations in temperature, pressure, external electric or magnetic fields, and chemical vapors as indicated in Ref. 44. The common strategy is to induce mesophase fixation in an appropriate matrix. Specific methods to achieve this goal include the following:

(a) Synthesis of side-chain or main-chain chiral nematic polymers that have the potential of forming a glassy matrix to "freeze" the requisite Grandjean texture.

(b) Photopolymerization of acrylate or methacrylate monomers, existing in a prescribed mesomorphic state, which contain cholesterol[45] or (hydroxypropyl)cellulose[46] as the pendant group.

(c) Photo-induced crosslinking of lyotropic mesophases consisting of poly(γ-butyl D- or L-glutamate) in triethylene glycol dimethacrylate, the latter serving both as a solvent and a crosslinker.[44,47]

Although both crosslinking and *in-situ* polymerization procedures are appealing to practical applications, the results are less than optimal. Notch filters (i.e., a pair of left- and right-handed devices stacked together) produced in this manner were found to possess an extinction of 0.2 to 0.8 optical density unit,[44,47] whereas the vitrification approach yields an extinction of 2.0 optical density units on substrates without surface treatment.[48] It appears that volume reduction, accompanying the curing process in general, contributes to the diminished extinction by destroying the alignment achieved in the fluid state.

Chiral Nematic Polymers

For electro-optic-device applications using field-induced molecular orientation, LC's function in the fluid state to offer a response time of the order of a millisecond. For the other two device concepts mentioned previously, a solid film is desirable in view of much-improved mesophase stability and environmental durability over a fluid film. In principle, an LC mesophase intended for an optical application can be frozen in a glassy matrix to avoid light scattering from grain boundaries present in a polycrystalline film. However, most LC's lack the ability to vitrify and, as a result, liquid crystalline polymers (LCP's) have attracted a great deal of attention in recent years. Several books and review articles have appeared on the fundamentals and potential applications of this class of optical materials.[49–53] Compared with LC's that tend to crystallize on cooling, LCP's are unique in that the particular mesophase desired can be frozen in the polymer matrix by first heating the sample close to the upper limit of the mesophase temperature range and then quenching it to below the glass transition temperature.

In regard to chemical structure, thermotropic LC polymers can be categorized into main-chain and side-chain polymers. Thermotropic LC polymers known to exhibit the cholesteric mesophase are surveyed in what follows.

1. Main-Chain Polymers

There exist numerous reports on thermotropic main-chain cholesteric LC polymers based on (*R*)-(+)-3-methyladipic acid[54–56] and chiral glycols and glycerols.[57,58] Tables 4 and 5 of Chap. 2 in Ref. 51 summarize the structures and mesomorphic properties of LC homopolymers and copolymers carrying the (*R*)-(+)-3-methyladipoyl group. The information available in the literature confirms the left-handed nature of these materials. No optical characterizations of thermotropic polymers containing chiral glycol and glycerol ethers have been reported, but the crystalline or semicrystalline character of these materials and their relatively high mesophase transition temperatures suggest that these materials are not likely to be suitable for optical device applications.

2. Polypeptides

It is well known that polypeptides, such as poly(γ-benzyl L-glutamate), exhibit lyotropic mesomorphism in a number of solvents;[54] however, their thermotropic behaviors have not been reported until recently by Watanabe *et al.*,[60–63] who presented several examples of derivatized poly(L-glutamate) exhibiting the cholesteric mesophase. Mesomorphism in these copolypeptides is believed to be due to the formation of mesogenic α-helices together with chiral perturbations on the backbone, while the flexible pendant groups serve as a solvent, as in a lyotropic system. According to Refs. 60–63, the helical sense of the cholesteric mesophase can be reversed by an inversion of chirality on the backbone. The potential of poly [(γ-benzyl L-glutamate)-co-(γ-dodecyl L-glutamate)], which shows cholesteric mesophase, as an optical material for device application was also appraised in our laboratory. It was found that the selective reflection wavelength is a relatively strong function of three parameters: temperature, comonomer ratio, and chain length, which combine to make this material extremely difficult to process into devices with reproducible optical properties. Furthermore, its low T_g, typically –20°C to –30°C, precludes the possibility of achieving long-term mesophase stability or application as a freestanding film.

3. Cellulose Derivatives

(Hydroxypropyl)cellulose, HPC, has been extensively studied because its mesomorphism can be realized in water and common organic solvents. Most cellulose derivatives display cholesteric mesophase in solution or bulk.[64–66] Optical characterization of the esters of HPC showed a right-handed helical structure. However, in our laboratory, the selective reflection of these thermotropic materials was found to be extremely weak with optical densities of less than 0.10 as compared to the theoretical limiting value of 0.30. The other disadvantage is the low T_g (<0°C), which prevents the Grandjean texture from being frozen in the glassy matrix.

4. Side-Chain Homopolymers

Freidzon *et al.*[67] reported acrylate homopolymers carrying cholesteryl pendant groups. The thermal characterization data showed a 2°C to 5°C temperature range for the existence of a cholesteric mesophase preceded by a smectic mesophase over a temperature range of up to 100°C, depending on the polymer molecular weight. In view of the fact that cholesterol-containing monomers are usually mesomorphic in their own right (typically cholesteric), it is not surprising that the desired cholesteric mesophase is overwhelmed by the higher-order smectic mesophase as a result of polymerization. Thus, it is advisable to explore chiral building blocks other than cholesterol. In fact, the first examples of cholesteric homopolymers using nonmesomorphic monomers containing (*S*)-2-methyl-1-butyloxy moiety and polysiloxane as the backbone have been successfully synthesized[68] and characterized to present a left-handed helical structure according to the commonly accepted convention.[69,70] The same chiral moiety was also employed to synthesize cholesteric homopolymers with a side-on attachment.[71] The fact that the selective reflection wavelength of homopolymers cannot be readily tuned by comonomer ratio, as is commonly achieved in copolymers, is expected to limit the practical applications in which the capability for wavelength tuning is desired.

5. Side-Chain Copolymers

Existing cholesteric side-chain copolymers have been extensively reviewed in Chap. 2 of Ref. 51 and Chap. 9 of Ref. 52. Typically, a nematogenic monomer, defined as one that by itself forms a nematic homopolymer, is copolymerized with a chiral, mesogenic, or nonmesogenic monomer to form a cholesteric side-chain copolymer. Although naturally occurring (–)-5-cholesten-3β-ol has been the most widely employed chiral precursor, it was found to consistently produce left-handed structures. The enantiomer of this naturally occurring cholesterol is expected to yield the right-handed counterpart, but it is not readily available, even though it has been successfully synthesized in the laboratory.[72] In addition to cholesterol, 1-phenylethylamine has also been successfully incorporated to produce cholesteric copolymer.[73] With several known nematogenic monomers, we have identified and synthesized new chiral comonomers derived from enantiomers of 1-phenylethylamine, 1-phenylethanol, 2-methoxy-2-phenylethanol, and methyl mandelate. The resultant copolymers are capable of forming the Grandjean texture with λ_R in the visible and near-infrared region. Key accomplishments are summarized as follows:

(a) Because of the availability of the enantiomers of these chiral precursors, both left- and right-handed chiral nematic copolymers were successfully synthesized.[74,75] The hitherto scarce right-handed materials have thus become available for the exploration of a variety of optical device concepts.

(b) A chiral/nematic molecular interaction model of a steric nature was successfully employed to elucidate the observed helical sense.[75] However, the applicability of this model is limited in scope, and more sophisticated molecular modeling is warranted.

(c) Helical sense observed in chiral nematic copolymers was found to be consistent with that of the low-molar-mass analogues, and helical twisting power was found to increase upon polymerization, although the effect appears to be system specific.[8]

(d) With an end-on attachment of a nematogenic rigid core to the polymer backbone, the smectic mesophase was found to predominate over the cholesteric mesophase as the *p*-phenylene ring system was replaced with *trans*-cyclohexylene counterpart.[76]

(e) The formation of Grandjean texture was found to be facilitated by moderating the polymer backbone flexibility within the acrylate and methacrylate-mixed backbone series without affecting the helical twisting power.[77]

More recently, cyanobiphenyl,[78] cyanotolan,[79] and cyanoterphenyl[80] groups were employed as high optical birefringence moieties for the synthesis of chiral nematic copolymers with a broader selective reflection band than achieved previously. Thermotropic and optical properties accompanied by chemical structures are illustrated in Tables 66.VI and 66.VII for cyanotolan- and cyanoterphenyl-containing systems, respectively. In the cyanotolan series, it is noted that for an increasing spacer length to the nematogen, T_g undergoes a monotonic decrease, whereas T_c shows an odd-and-even effect. Within the same spacer length of 4 at an increasing chiral mole fraction, T_g stays reasonably constant while a pronounced depression in T_c is observed, which is also the case with the cyanoterphenyl series. The selective wavelength reflection scans of Copolymer (I) with $n = 4$ and $x = 0.07$ and Copolymer (II) with $x = 0.10$ are reproduced in Fig. 66.55 to demonstrate the broadband characteristic.

Low-Molar-Mass Glass-Forming Systems

Because of their fluid nature and low viscosity, low-molar-mass LC's are capable of forming uniform films with a high degree of mesomorphic ordering. However, as indicated earlier, there are several obvious disadvantages: a lack of environmental durability and long-term mesophase stability, and the inability to vitrify in general. These problems can be

Table 66.VI: Thermal and optical properties and molecular weights of chiral nematic copolymers containing cyanotolan and 1-phenylethanol as pendant groups.

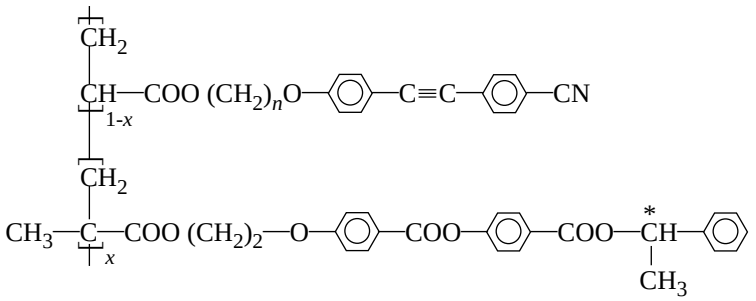

(I)

Spacer	Chiral x	Phase Transition[a] (°C)	ΔC_p (W/g)	ΔH_c (J/g)	$\overline{M}_w$	$\overline{M}_w/\overline{M}_n$	λ_R (nm)
2	0.05	G 76 Ch 112 I	0.16	2.5	11,900	1.7	840
3	0.05	G 58 Ch 85 I	0.13	0.5	8,980	1.6	(b)
4	0.05	G 45 Ch 117 I	0.14	1.7	12,200	2.3	920
4	0.07	G 43 Ch 104	0.13	1.3	10,800	2.3	770
4	0.13	G 48 Ch 94	0.13	1.4	13,700	2.2	450
6	0.08	G 34 Ch 116 I	0.18	2.0	17,500	2.1	1140

(a) G: glass; Ch: cholesteric; I: isotropic.

(b) The cholesteric mesophase was identified with polarizing optical microscopy, but the selective wavelength reflection property could not be determined because of the relatively narrow mesophase temperature range that prevents adequate molecular alignment from being achieved via annealing.

Table 66.VII: Thermal and optical properties and molecular weights of chiral nematic copolymers containing cyanoterphenyl and 1-phenylethylamine as pendant groups.

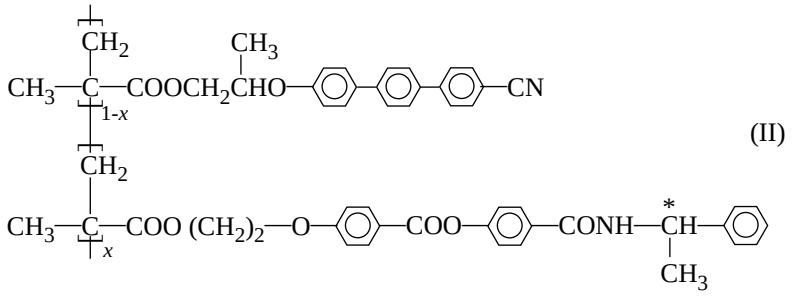

Chiral x	Phase Transition[a] (°C)	ΔC_p (W/g)	ΔH_c (J/g)	$\overline{M}_w$	$\overline{M}_w/\overline{M}_n$	λ_R (nm)
0.051	G 117 Ch 201 I	0.24	0.83	15,000	3.4	1,100
0.064	G 113 Ch 193 I	0.23	0.39	11,000	3.0	786
0.10	G 112 Ch 181 I	0.25	0.57	6,500	2.1	634
0.12	G 120 Ch 173 I	0.27	0.42	6,100	3.1	510

[a] G: glass; Ch: cholesteric; I: isotropic.

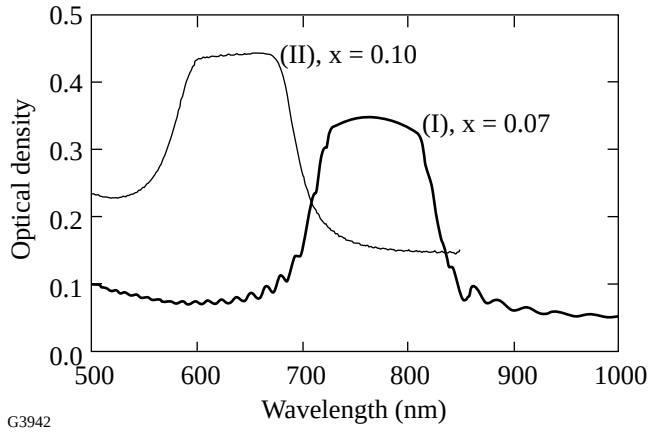

Figure 66.55
UV-visible spectra (i.e., selective wavelength reflection scans) of Copolymer (I) with $n = 4$ and $x = 0.07$ and Copolymer (II) with $x = 0.10$.

overcome by glass-forming polymeric LC's. Nevertheless, their generally high melt or solution viscosity tends to cause difficulty in processing these materials into well-aligned, uniform thin films. To circumvent all these practical problems, glassy low-molar-mass liquid crystals (GLMLC's) have emerged as a novel class of optical materials with a great deal of potential. These materials are composed of relatively small molecules with molecular weights less than 2,000. Because of their relatively low melt viscosity, it is relatively easy to form GLMLC's into large, uniform films with the desired mesophase frozen into the glassy state, thus producing an environmentally robust optical device. Since polymerization is not involved in the synthesis of GLMLC's, the availability of these materials will not be limited by the polymerizability problem as encountered with some functional monomers.

Though glass formation in small organic molecules has long been recognized,[81–85] it was not until the 1980's that active investigations of GLMLC's were resumed.[86–91] The fact that melting and crystallization peaks were observed in many of the reported differential scanning calorimetry (DSC) scans suggests that they are semicrystalline or prone to thermally induced crystallization, and thus would not be appropriate for optical device applications. In the past few years significant advances in GLMLC's have been witnessed, presumably because of the general interest in exploring organic materials for electro-optical as well as optoelectronic applications. In terms of molecular structure, GLMLC's can be classified into acyclics[86–97] and cyclics.[98–117] Acyclic compounds have been reviewed by Wedler *et al.*;[95] structurally, they carry either one or two strings. As encountered in LCP's, there are both main-chain and side-chain cyclic oligomers. Main-chain cyclic oligomers were first reported by Percec *et al.*[111–113] Side-chain cyclic oligomers include cyclophosphazene and cyclosiloxane LC's. It is noted that few cyclophos-phazene LC's show a glass transition.[114–117]

Of all the low-molar-mass glass-forming liquid crystals, cyclosiloxane LC's have been the most widely investigated following the 1981 patent of Kreuzer *et al*.[98] They are essentially cyclic analogues of side-chain siloxane polymers. Even though cyclic siloxane LC's have only 4 to 7 monomeric units, they exhibit glass transition and clearing temperatures that are generally close to[110] but in some cases[104] very different from their long-chain counterparts. A variety of mesogenic moieties have been successfully incorporated to induce the desired glass-forming and mesomorphic properties with a glass transition temperature of up to 80°C.[118] However, thus far no mesogens with an extended π-conjugation have been successfully incorporated, and no chiral moieties other than cholesterol have been attempted to induce chirality. Nevertheless, numerous potential applications of cyclosiloxanes have been explored: environmentally robust notch filter,[48] optical information storage,[103,109,119] and nonlinear optics.[120,121]

Carbocyclic Glass-Forming Chiral Nematics

Conceptually, GLMLC's represent a balance between two seemingly opposing trends: one to discourage crystallization and the other to encourage LC mesomorphism. Simply put, a delicate balance between order and disorder must be struck. The question of why certain materials are more inclined to glass formation than others has remained unanswered in glass science to date. In principle, molecular systems with a strong temperature dependence of free volume tend to vitrify upon cooling at a rate sufficiently rapid in comparison to molecular relaxation processes. Nevertheless, the implementation of this concept in molecular design is made difficult by a general lack of understanding of glass formation by organic compounds.

In search of new, alternative glass-forming liquid crystals as advanced organic materials, we have explored a novel molecular design concept in which two opposing structural features are chemically bonded via a flexible spacer, one a mesogenic group and the other a diametrically different moiety. The idea is to suppress one's tendency to crystallize by having the other present an excluded-volume effect. Since mesogenic molecules are typically structurally rigid and elongated in shape, their counterpart, referred to as the central core, should preferably be bulky and nonplanar in shape. A knowledge base exists for the design of mesogens. The central core is less understood, but it should preferably assume one of the following structures: aliphatic cyclics, bicyclics, or tricyclics. The length of the flexible spacer linking the two plays a critical role in effecting the synergy with which vitrification and mesomorphism can be accomplished without residual crystallinity or tendency toward crystallization. Stereochemical features presented by the central core may also influence the ease of glass formation as well as morphological stability. In addition to mesogens, chiral groups can also be attached to the central core to induce cholesteric mesomorphism.

In a recent series of papers,[122–124] we have reported novel glassy liquid crystals derived from 1,3,5-cyclohexanetricarboxylic and (1*R*,3*S*)-(+)-camphoric acids. Three approaches were demonstrated to be capable of inducing cholesteric mesomorphism: chiral nematic cyclic oligomer, nematogenic group attached to a chiral ring, and chiral/nematic mixture with the chemical structures shown in Fig. 66.56 and the relevant properties summarized in Table 66.VIII. Although Compound (IV) is nonmesogenic, its mixture with (III) at $x = 0.62$ yields a cholesteric mesophase. The selective wavelength properties of Compounds (V) and (VI) together with that of the mixture (IV)/(III) are displayed in Fig. 66.57. Nematic compounds [(VII) and (VIII)] and their chiral dopants [(IX) through (XIII)], as depicted in Fig. 66.58, were designed to provide new insight into the induced cholesteric mesomorphism. The observed thermotropic properties and optical properties are compiled in Table 66.IX. Note that all the resultant chiral nematic mixtures are capable of vitrification, with glass transitions occurring above the ambient, and show selective wavelength reflection in the visible and near-

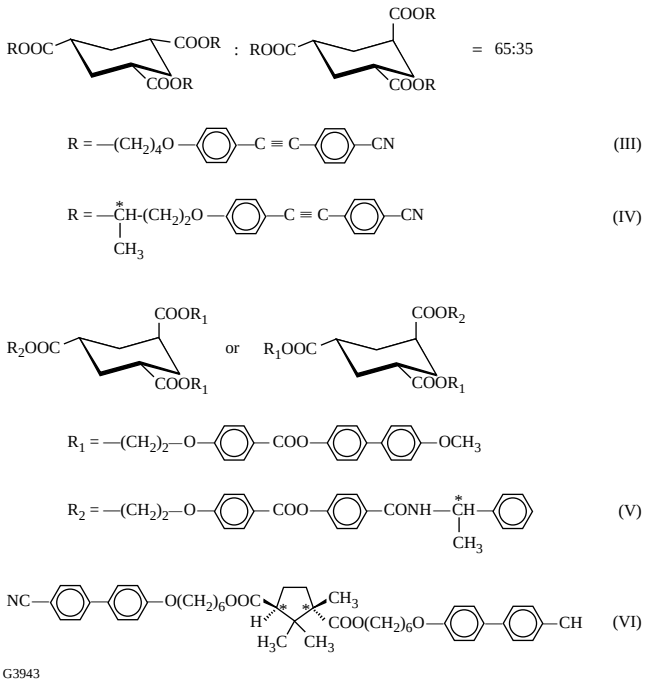

Figure 66.56
Chemical structures of Compounds (III) through (VI).

Table 66.VIII: Thermotropic and selective reflection properties of Compounds (III) through (VI).

System	Phase Transition[a] (°C)	ΔC_p (W/g)	ΔH_c (J/g)	λ_R (nm)
(III)	G 28 N 124 I	0.18	3.33	NA
(IV)	G 33 I	0.19	NA	NA
(IV)/(III), $x = 0.62$	G 36 Ch 85 I	0.19	1.73	1355
(V), $x = 0.33$	G 69 Ch 137 I	0.12	0.46	425
(VI), $x = 0.50$	G −5 Ch 42 I	0.16	2.86	1716

[a] G: glass; N: nematic; Ch: cholesteric; I: isotropic.

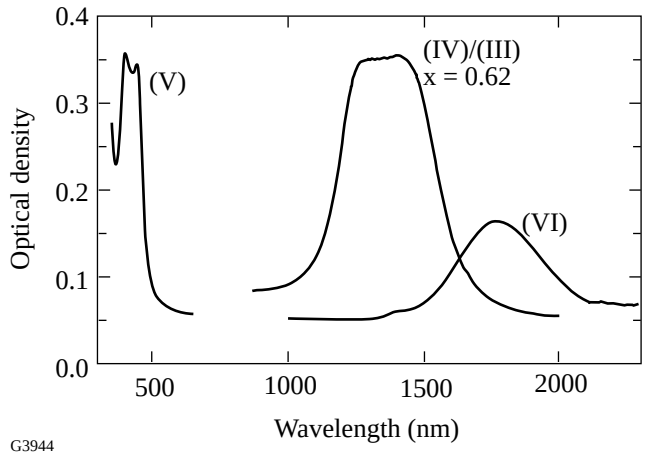

Figure 66.57
UV-visible spectra (i.e., selective wavelength reflection scans) of Compounds (V), (VI), and (IV)/(III) with $x = 0.62$.

infrared region. Furthermore, the handedness of the cholesteric mesomorphism, in relation to the absolute configuration of the chiral precursor and the value of HTP, can be accounted for by a molecular interaction model of a steric origin. The molecular environment surrounding the chiral center is depicted in Fig. 66.59, in which a benzene or naphthalene ring serves as an anchoring plane. The predictions of a left-handed cholesteric mesomorphism resulting from an absolute configuration *S*, and of a higher HTP value with naphthalene ring as an anchor compared to benzene ring, are both borne out by the experimental observations presented in Table 66.IX.[124] As demonstrated in Fig. 66.60, chiral nematic mixtures (IX)/(VII) and (XIII)/(VII), both with $x = 0.16$, possess a broad selective reflection band with pronounced side-band oscillations, a manifestation of the ease of processing into highly uniform films of which their polymeric counterparts are normally incapable.

Morphological Stability of Low-Molar-Mass Glass-Forming Systems

Since a typical quenched glass lies in a nonequilibrium state, it is suspected that thermally activated phase transformation (e.g., crystallization) may occur given sufficient energy and time. Crystallization from a glassy film is detrimental to device performance in view of light scattering from grain boundaries and deteriorating contact at an interface. In essence, the morphological stability of an LC glass determines a device's useful lifetime. Similarly, the morphological stability of an LC mesophase above T_g is critical to the optimization of a device-manufacturing process in which thermal annealing is normally performed to maximize the degree of ordering. In this process, the desired mesophase may yield to an energetically favored (meso)phase, as we have reported recently.[125] The reason is that the formation of an energetically favored (meso)phase may escape detection by standard techniques with finite scanning rates, such as differential scanning calorimetry and hot-stage polarized optical microscopy. Thus, for an LC glass to be useful in practice, it is imperative that morphological stability at temperatures both below and above T_g be addressed. In fact, crystallization from mesomorphic and isotropic melts of thermotropic LC polymers[126,127] and from isotropic melts of nonmesogenic, low-molar-mass materials[128] has been observed and its kinetics intensively investigated in recent years. While the main theme of this review is chiral nematic systems, we embarked on an investigation of morphological stability of glass-forming nematics with the anticipation that chiral nematic systems would be more stable than nematics because of the enhanced structural dissimilarity between pendant groups. Our investigation to date has concluded that when annealed at any temperature between T_g and T_m (crystalline melting point) for a period of up to a few months, most chiral nematics listed in Tables 66.VIII and 66.IX showed no evidence of crystal-

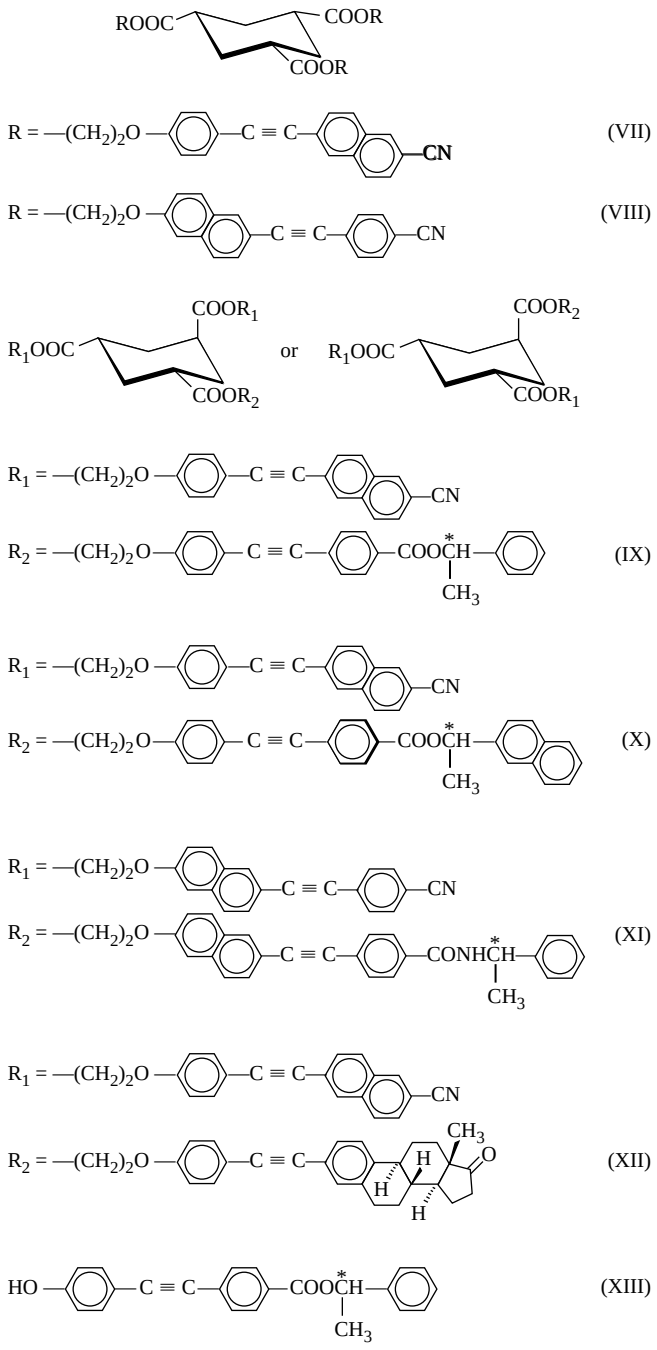

Figure 66.58
Chemical structures of Compounds (VII) through (XIII).

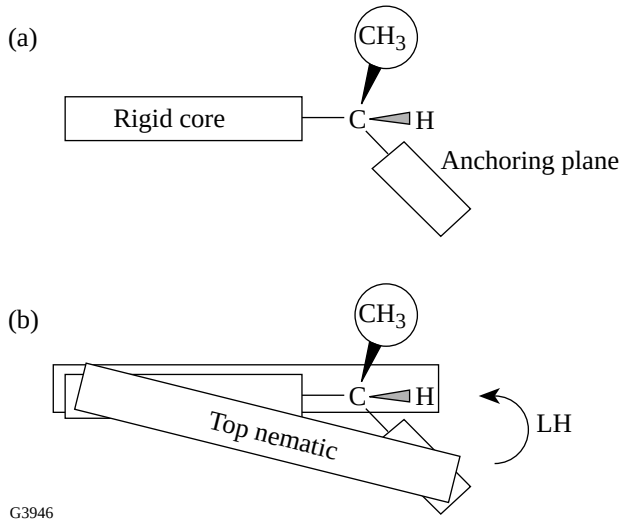

Figure 66.59
Chiral/nematic molecular interaction model: (a) chiral pendant group with an absolute configuration *S*; (b) helical twisting of the top nematic sublayer by the methyl group protruding from an asymmetric carbon center.

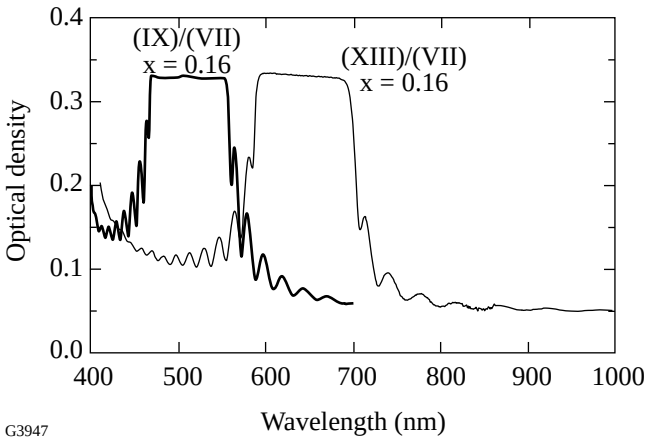

Figure 66.60
UV-visible spectra (i.e., selective wavelength reflection scans) of (IX)/(VII) on a single glass substrate and (XIII)/(VII) sandwiched between a pair of substrates, both with $x = 0.16$.

Table 66.IX: Thermotropic and optical properties of chiral nematic mixtures (VII) and (VIII) doped with (IX) through (XIII).

System	x [a]	λ_R (nm)	Phase [b] Transition(°C)	ΔC_p (W/g)	ΔH_c (J/g)	Absolute Configuration of Chiral Precursor	Handedness of Cholesteric Mesophase	10^{-4} HTP (nm^{-1})
(VII)	0.00	NA	G 60 N 197 I	0.13	2.72			
(VIII)	0.00	NA	G 65 N 191 I	0.12	2.46			
(IX)/(VII)	0.33 0.16 0.12 0.08	(c) 508 713 1024	G 61 Ch 77 I G 62 Ch 136 I G 62 Ch 155 I G 62 Ch 169 I	0.16 0.15 0.15 0.15	0.34 1.00 1.51 1.36	*S*	LH	203±3
(X)/(VII)	0.33 0.08 0.06 0.04	(d) 545 720 1070	G 70 I G 60 Ch 164 I G 60 Ch 171 I G 61 Ch 182 I	0.12 0.10 0.11 0.11	NA 2.29 1.97 2.19	*R*	RH	387±2
(XI)/(VIII)	0.33 0.20 0.14 0.09	(c) 580 880 1525	G 81 Ch 106 I G 70 Ch 132 I G 68 Ch 147 I G 66 Ch 163 I	0.12 0.11 0.11 0.14	0.47 1.30 1.20 0.69	*R*	RH	137±3
(XII)/(VII)	0.33 0.25 0.20	930 1225 1770	G 79 Ch 182 I G 72 Ch 179 I G 70 Ch 189 I	0.13 0.12 0.16	1.84 1.68 1.02	(e)	LH	53±2
(XIII)/(VII)	1.00 0.16 0.12 0.08	(d) 633 800 1160	G 28 I G 50 Ch 128 I G 51 Ch 149 I G 52 Ch 163 I	0.20 0.12 0.13 0.13	NA 1.03 1.62 1.21	*S*	LH	171±3

(a) x is defined as the number of chiral side arms divided by the total number of nematic and chiral side arms in the blend.
(b) G: glass; N: nematic; Ch: cholesteric; I: isotropic.
(c) Showing cholesteric oily streaks under polarizing optical microscope, but no selective reflection peaks available for determination of λ_R because of close proximity of T_c to T_g.
(d) Nonmesogenic.
(e) Unspecified.

lization. On the contrary, the crystallization rate is experimentally accessible in nematics that were selected for an investigation of morphological stability to identify relevant structural parameters.

We have offered a definitive basis for assessing morphological stability[129] of glass-forming liquid crystals as a novel class of advanced organic materials. Model compounds depicted in Fig. 66.61 were synthesized and their stereochemical characteristics determined by proton-NMR spectroscopy. The morphological stability was evaluated using the measurement of crystallization velocity CV, defined as the linear spherulitic growth rate, as a function of temperature between T_g and T_m, as plotted in Fig. 66.62. It was found that (a) an *all-equatorial* configuration enhances morphological stability over an *all-axial* configuration by two orders of magnitude with cyanotolan as the pendant mesogenic core; (b) morphological stability is largely unaffected by the spacer length connecting the mesogenic group to the central core, although both T_g and T_m are depressed, whereas T_c is significantly elevated by a longer spacer; (c) as cyanotolan is replaced by 1-phenyl-2-(6-cyanonaphth-2-yl)ethyne as a stronger nematogen in terms of transition temperatures and mesophase temperature range, the morphological stability was found to diminish by almost an order of magnitude; and (d) mixed *equatorial-axial* modes increase morphological stability over both *all-equatorial* and *all-axial* modes to such an extent that the morphological stability turns out to be comparable to isotactic polystyrene, a typical "slowly crystallizing" polymer, with a maximum CV of the order of 10 nm/s.

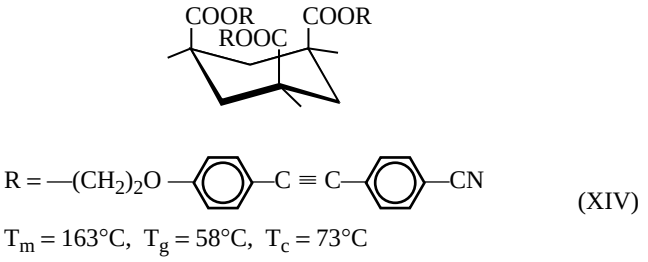

Figure 66.61
Chemical structures of (XIV) through (XVIII) plus (VII) selected for an investigation of morphological stability against crystallization.

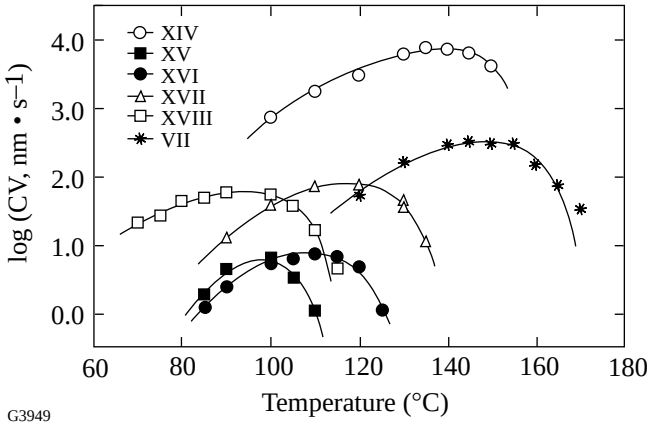

Figure 66.62
Crystallization velocity, CV, as a function of temperature of the model compounds shown in Fig. 66.61 to display the effects of stereochemistry, mesogenic core, and spacer length. The curves represent the best fit to the secondary nucleation theory.

Summary and Future Outlook

The unique property of chiral nematic liquid crystals to produce selective wavelength reflection accompanied by circular polarization has potential applications in numerous optical devices, such as notch filters, beamsplitters, circular polarizers, etc., as well as optical information processing, storage, and display. The main theme of this review is on materials capable of vitrification into cholesteric glasses as a way to preserve mesogenic order, thereby facilitating practical applications. With a glass transition temperature above the ambient, free-standing films may become a reality. Recent advances in chiral nematic side-chain polymeric and low-molar-mass systems are surveyed. Theories of optical birefringence and selective reflection bandwidth are outlined to furnish a basis for optimizing bandwidth with respect to the number of delocalized π-electrons. A wide variety of polymeric systems have been reported over the past three decades, and we have presented new systems incorporating high optical birefringence nematogenic and chiral pendant groups to increase the selective reflection bandwidth.

Because of the demonstrated capability for vitrification and relative ease of processing into uniform thin films, we have focused on the design and synthesis of low-molar-mass systems with morphological stability comparable to typical "slowly crystallizing" polymers. The underlying molecular design concept is also potentially instrumental to the development of a diversity of functional organic materials. From a practical perspective, novel systems with selective reflection occurring in the visible and infrared spectral region with a broad and

narrow bandwidth and an elevated glass transition temperature are of interest. Moreover, processing techniques capable of producing defect-free thin films, including freestanding ones, are crucial to bringing this class of optical materials to fruition.

From a fundamental perspective, a molecular interaction model of a steric origin is capable of relating helical sense of cholesteric mesomorphism to absolute configuration of the chiral precursor within a series of structurally similar systems. Nonetheless, the interpretation of helical sense and twisting power in terms of chemical structure remains as challenging as ever, despite all the theoretical and computational efforts devoted to chiral nematic systems over the last four decades. It is hoped that an appropriate theory governing the interaction between light and condensed matter, coupled with intensive computation accounting for realistic atomic and molecular interactions, will lead to a better understanding of the structure-property relationships and, hence, improved materials for practical applications.

ACKNOWLEDGEMENT

The authors wish to express their gratitude to Professor Andrew S. Kende of the Chemistry Department of the University of Rochester for his advice on organic synthesis, to Dr. Stephen D. Jacobs, Dr. Ansgar Schmid, and Mr. Kenneth L. Marshall for helpful discussions and technical assistance. The early phase of this research was supported with an Expedited Award from NSF under CTS-8714924 and by the Petroleum Research Fund administered by the American Chemical Society. The authors also wish to acknowledge the support by Kaiser Electronics in San Jose, California, by the National Science Foundation under CTS-9500737 and an engineering research equipment grant CTS-9411604, and by the Ministry of International Trade and Industry of Japan. In addition, our liquid crystal materials research was supported in part by the U.S. Department of Energy, Division of Inertial Confinement Fusion under Cooperative Agreement No. DE-FC03-92SF19460 with the Laboratory for Laser Energetics at the University of Rochester. The support of DOE does not constitute an endorsement by DOE of the views expressed in this article.

REFERENCES

1. W. H. de Jeu, *Physical Properties of Liquid Crystalline Materials* (Gordon and Breach, New York, 1980).
2. H. Finkelmann, in *Thermotropic Liquid Crystals*, edited by G. W. Gray (Wiley, New York, 1987), p. 145.
3. E. B. Priestley, in *Introduction to Liquid Crystals*, edited by E. B. Priestley, P. J. Wojtowicz, and P. Sheng (Plenum Press, New York, 1975), p. 1.
4. I. Sage, in *Thermotropic Liquid Crystals*, edited by G. W. Gray (Wiley, New York, 1987).
5. S.-T. Wu, in *Optical Materials: A Series of Advances*, edited by S. Musikant (Marcel Dekker, New York, 1990), Vol. 1, Chap. 1.
6. I.-C. Khoo and S.-T. Wu, *Optics and Nonlinear Optics of Liquid Crystals*, Nonlinear Optics, Vol. 1 (World Scientific, Singapore, 1993).
7. M. Schadt, Ber. Bunsenges. Phys. Chem. **97**, 1213 (1993).
8. S. D. Jacobs, K. A. Cerqua, K. L. Marshall, A. Schmid, M. J. Guardalben, and K. J. Skerrett, J. Opt. Soc. Am. B **5**, 1962 (1988).
9. K. Hirabayashi and T. Kurokawa, Liq. Cryst. **14**, 307 (1993).
10. D. A. McL. Smith and H. J. Coles, Liq. Cryst. **14**, 937 (1993).
11. G. Solladié and R. G. Zimmermann, Angew. Chem. Int. Ed. Engl. **23**, 348 (1984).
12. H. Baessler and M. M. Labes, J. Chem. Phys. **52**, 631 (1970).
13. H. Stegemeyer and K.-J. Mainusch, Chem. Phys. Lett. **6**, 5 (1970).
14. J. W. Goodby, J. Mater. Chem. **1**, 307 (1991).
15. A. J. Slaney *et al.*, J. Mater. Chem. **2**, 805 (1992).
16. G. W. Gray and D. G. McDonnell, Mol. Cryst. Liq. Cryst. Lett. **34**, 211 (1977).
17. N. Emoto *et al.*, Jpn. J. Appl. Phys. **28**, L 121 (1989).
18. S. Krishnamurthy and S.-H. Chen, Macromolecules **25**, 4485 (1992).
19. J. W. Goodby *et al.*, J. Am. Chem. Soc. **108**, 4729 (1986).
20. G. Gottarelli, B. Samori, and C. Stremmenos, Chem. Phys. Lett. **40**, 308 (1976).
21. G. Gottarelli *et al.*, Tetrahedron **37**, 395 (1981).
22. W. H. Pirkle and P. L. Rinaldi, J. Org. Chem. **45**, 1379 (1980).
23. P. L. Rinaldi, M. S. R. Naidu, and W. E. Conaway, J. Org. Chem. **47**, 3987 (1982).
24. P. L. Rinaldi and M. Wilk, J. Org. Chem. **48**, 2141 (1983).
25. G. S. Chilaya and L. N. Lisetski, Mol. Cryst. Liq. Cryst. **140**, 243 (1986).
26. L. Varichon, A. Ten Bosch, and P. Sixou, Liq. Cryst. **9**, 710 (1991).
27. L. N. Lisetski and A. V. Tolmachev, Liq. Cryst. **5**, 877 (1989).
28. L. A. Kutulya *et al.*, J. Phys. Org. Chem. **5**, 308 (1992).
29. W. J. A. Goossens, Mol. Cryst. Liq. Cryst. **12**, 237 (1971).
30. M. R. Wilson and M. P. Allen, Mol. Cryst. Liq. Cryst. **198**, 465 (1991).
31. M. P. Allen and M. R. Wilson, J. Comput.-Aided Mol. Des. **3**, 335 (1989).
32. D. A. Dunmur and M. R.Wilson, Mol. Simul. **4**, 37 (1989).
33. S. S. Patnaik *et al.*, Liq. Cryst. **19**, 213 (1995).

34. R. Memmer, H.-G. Kuball, and A. Schönhofer, Ber. Bunsenges. Phys. Chem. **97**, 1193 (1993).

35. R. Memmer, H.-G. Kuball, and A. Schönhofer, Liq. Cryst. **15**, 345 (1993).

36. M. R. Wilson and D. A. Dunmur, Liq. Cryst. **5**, 987 (1989).

37. D. G. McDonnell, in *Thermotropic Liquid Crystals*, edited by G. W. Gray (Wiley, New York, 1987), p. 120.

38. H. F. Gleeson and H. J. Coles, Mol. Cryst. Liq. Cryst. **170**, 9 (1989).

39. HL. De Vries, Acta Cryst. **4**, 219 (1951).

40. H. Finkelmann, in *Liquid Crystallinity in Polymers: Principles and Fundamental Properties*, edited by A. Ciferri (VCH Publisher, New York, 1991), p. 329.

41. S.-T. Wu, U. Finkenzeller, and V. Reiffenrath, J. Appl. Phys. **65**, 4372 (1989); S.-T. Wu, E. Ramos, and U. Finkenzeller, J. Appl. Phys. **68**, 78 (1990).

42. M. Hird *et al.*, Liq. Cryst. **15**, 123 (1993).

43. S.-T. Wu, Phys. Rev. A **33**, 1270 (1986).

44. S. Ishihara *et al.*, Polymer **29**, 2141 (1988).

45. P. J. Shannon, Macromolecules **17**, 1873 (1984).

46. S. N. Bhadani and D. G. Gray, Mol. Cryst. Liq. Cryst. Lett. **102**, 255 (1984).

47. T. Tsutsui and R. Tanaka, Polymer **21**, 1351 (1980).

48. M. L. Tsai, S. H. Chen, and S. D. Jacobs, Appl. Phys. Lett. **54**, 2395 (1989).

49. A. Blumstein, ed. *Liquid Crystalline Order in Polymers* (Academic Press, New York, 1978).

50. N. A. Platé, ed. *Advances in Polymer Science* (Springer-Verlag, Berlin, 1984), Vols. 59 and 60/61.

51. L. L. Chapoy, ed. *Recent Advances in Liquid Crystalline Polymers* (Elsevier, London, 1985).

52. C. B. McArdle, ed. *Side Chain Liquid Crystal Polymers* (Chapman and Hall, New York, 1989).

53. A. Ciferri, ed. *Liquid Crystallinity in Polymers* (VCH Publishers, New York, 1991).

54. H. Hara *et al.*, Macromolecules **21**, 14 (1988).

55. J. Watanabe and W. R. Krigbaum, Mol. Cryst. Liq. Cryst. **135**, 1 (1986).

56. W. R. Krigbaum *et al.*, Mol. Cryst. Liq. Cryst. **76**, 79 (1981).

57. E. Chiellini, P. Nieri, and G. Galli, Mol. Cryst. Liq. Cryst. **113**, 213 (1984).

58. E. Chiellini and G. Galli, Macromolecules **18**, 1652 (1985).

59. D. B. DuPré and E. T. Samulski, in *Liquid Crystals: The Fourth State of Matter*, edited by F. D. Seava (Marcel Dekker, New York, 1979), p. 203.

60. J. Watanabe *et al.*, Macromolecules **17**, 1004 (1984).

61. J. Watanabe *et al.*, Macromolecules **18**, 2141 (1985).

62. J. Watanabe, M. Goto, and T. Nagase, Macromolecules **20**, 298 (1987).

63. J. Watanabe and T. Nagase, Macromolecules **21**, 171 (1988).

64. S.-L. Tseng, G. V. Laivins, and D. G. Gray, Macromolecules **15**, 1262 (1982).

65. G. V. Laivins and D. G. Gray, Macromolecules **18**, 1753 (1985).

66. L. Rusig *et al.*, J. Polym. Sci. B, Polym. Phys. **32**, 1907 (1994).

67. Y. S. Freidzon *et al.*, Makromol. Chem., Rapid Commun. **6**, 625 (1985).

68. H. Finkelmann and G. Rehage, Makromol. Chem., Rapid Commun. **3**, 859 (1982).

69. M. Born and E. Wolf, *Principles of Optics: Electromagnetic Theory of Propagation, Interference and Diffraction of Light*, 4th ed. (Pergamon Press, New York, 1970), Chap. 1.

70. H. Kozawaguchi and M. Wada, Mol. Cryst. Liq. Cryst. **45**, 55 (1978).

71. R. A. Lewthwaite, G. W. Gray, and K. J. Toyne, J. Mater. Chem. **2**, 119 (1992).

72. D. E. Mickus, D. G. Levitt, and S. D. Rychnovsky, J. Am. Chem. Soc. **114**, 359 (1992).

73. H. Finkelmann, J. Koldehoff, and H. Ringsdorf, Angew. Chem. Int. Ed. Engl. **17**, 935 (1978).

74. M. L. Tsai and S. H. Chen, Macromolecules **23**, 1908 (1990).

75. S. Krishnamurthy and S.-H. Chen, Macromolecules **24**, 3481 (1991).

76. S. Krishnamurthy, S.-H. Chen, and T. N. Blanton, Macromolecules **25**, 5119 (1992).

77. S. Krishnamurthy and S.-H. Chen, Macromolecules **24**, 4472 (1991).

78. J. C. Mastrangelo and S.-H. Chen, Macromolecules **26**, 6132 (1993).

79. H. Shi and S.-H. Chen, Macromolecules **26**, 5840 (1993).

80. J. C. Mastrangelo and S. H. Chen, Macromolecules, to be submitted.

81. B. Rosenberg, J. Chem. Phys. **31**, 238 (1959).

82. D. J. Plazek and J. H. Magill, J. Chem. Phys. **45**, 3038 (1966).

83. K. Tsuji, M. Sorai, and S. Seki, Bull. Chem. Soc. Jpn. **44**, 1452 (1971).

84. M. Sorai and S. Seki, Bull. Chem. Soc. Jpn. **44**, 2887 (1971).

85. M. Sorai and S. Seki, Mol. Cryst. Liq. Cryst. **23**, 299 (1973).

86. J. Grebovicz and B. Wunderlich, Mol. Cryst. Liq. Cryst. **76**, 287 (1981).

87. H. Yoshioka, M. Sorai, and H. Suga, Mol. Cryst. Liq. Cryst. **95**, 11 (1983).

88. K. S. Kunihisa and Y. Satomi, Mol. Cryst. Liq. Cryst. **141**, 1 (1986).

89. W. Weissflog and D. Demus, Liq. Cryst. **3**, 275 (1988).

90. W. Weissflog *et al.* Liq. Cryst. **5**, 111 (1989).

91. H. Dehne *et al.*, Liq. Cryst. **6**, 47 (1989).

92. W. Schafer *et al.*, Mol. Cryst. Liq. Cryst. **191**, 269 (1990).

93. R. Stannarius *et al.*, Liq. Cryst. **9**, 285 (1991).

94. H. J. Eichler *et al.*, Mol. Cryst. Liq. Cryst. **223**, 159 (1992).

95. W. Wedler *et al.*, J. Mater. Chem. **1**, 347 (1991).

96. W. Wedler *et al.*, J. Mater. Chem. **2**, 1195 (1992).

97. G. Attard and C. T. Imrie, Liq. Cryst. **11**, 785 (1992).

98. F.-H. Kreuzer *et al.*, E. P. Patent No. 60,335 (22 September 1982).

99. D. Makow, Mol. Cryst. Liq. Cryst. **123**, 347 (1985).

100. B. Hahn and V. Percec, Mol. Cryst. Liq. Cryst. Inc. Nonlin. Opt. **157**, 125 (1988).

101. V. Percec and B. Hahn, J. Polym. Sci. A, Polym. Chem. **27**, 2367 (1989).

102. H.-J. Eberle, A. Miller, and F.-H. Kreuzer, Liq. Cryst. **5**, 907 (1989).

103. R. Ortler *et al.*, Makromol. Chem., Rapid Commun. **10**, 189 (1989).

104. R. D. C. Richards *et al.*, J. Chem. Soc. Chem. Commun., 95 (1990).

105. F.-H. Kreuzer *et al.*, Mol. Cryst. Liq. Cryst. **199**, 345 (1991).

106. T. J. Bunning *et al.*, Liq. Cryst. **10**, 445 (1991).

107. T. J. Bunning *et al.*, Liq. Cryst. **16**, 769 (1994).

108. M. Ibn-Elhaj *et al.*, Liq. Cryst. **19**, 373 (1995).

109. L. V. Natarajan *et al.*, Adv. Mater. Opt. Electron. **1**, 293 (1992).

110. T. J. Bunning *et al.*, Mol. Cryst. Liq. Cryst. **231**, 163 (1993).

111. V. Percec and M. Kawasumi, Adv. Mater. **4**, 572 (1992).

112. V. Percec *et al.*, Macromolecules **25**, 3851 (1992).

113. V. Percec and M. Kawasumi, Liq. Cryst. **13**, 83 (1993).

114. Y. S. Freidzon *et al.*, Polymer Preprints **34**, 146 (1993).

115. R. E. Singler *et al.*, Macromolecules **20**, 1727 (1987).

116. H. R. Allcock and C. Kim, Macromolecules **22**, 2596 (1989).

117. K. Moriya, S. Yano, and M. Kajiwara, Chem. Lett., 1039 (1990).

118. K. D. Gresham *et al.*, J. Polym. Sci. A, Polym. Chem. **32**, 2039 (1994).

119. J. Pinsl, Chr. Bräuchle, and F.-H. Kreuzer, J. Mol. Electron. **3**, 9 (1987).

120. D. M. Walba *et al.*, Polymer Preprints **34**, 697 (1993).

121. H. Anneser *et al.*, Adv. Mater. **5**, 556 (1993).

122. H. Shi and S.-H. Chen, Liq. Cryst. **17**, 413 (1994).

123. H. Shi and S.-H. Chen, Liq. Cryst. **18**, 733 (1995).

124. H. Shi and S.-H. Chen, Liq. Cryst. **19**, 849 (1995).

125. J. C. Mastrangelo, T. N. Blanton, and S. H. Chen, Appl. Phys. Lett. **66**, 2212 (1995).

126. I. Campoy *et al.* Macromolecules **25**, 4392 (1992).

127. S. R. Zhao, A. Schaper, and W. Ruland, Acta Polym. **44**, 173 (1993).

128. K. Naito and A. Miura, J. Phys. Chem. **97**, 6240 (1993).

129. H. Shi and S. H. Chen, Liq. Cryst. **19**, 785 (1995).